Defence Research and Development Canada
Recherche et développement pour la défense Canada

DEFENCE R&D DÉFENSE

Ship Detection Performance of a High Frequency Hybrid Sky-Surface Wave Radar

R.J. Riddolls

Defence R&D Canada – Ottawa
TECHNICAL MEMORANDUM
DRDC Ottawa TM 2007-327
December 2007

Canada

Ship Detection Performance of a High Frequency Hybrid Sky-Surface Wave Radar

R. J. Riddolls
Defence R&D Canada – Ottawa

Defence R&D Canada – Ottawa
Technical Memorandum
DRDC Ottawa TM 2007-327
December 2007

Principal Author

Original signed by R. J. Riddolls

R. J. Riddolls

Approved by

Original signed by D. Dyck

D. Dyck
Head/Radar Systems Section

Approved for release by

Original signed by P. Lavoie

P. Lavoie
Head/Document Review Panel

Abstract

A high frequency radar configuration consisting of a skywave transmit path and a surface wave receive path is presented and analyzed. Limits on the radar resolution capability are determined using an analytic ray tracing formulation of radar signal propagation in an ionospheric plasma. This resolution is then substituted into the radar equation. It is found that the detection of low-velocity surface vessels is limited by ocean clutter. In this clutter-limited detection mode, it is found that the minimum detectable vessel radar cross section (RCS) depends on the direction of the wind relative to the radar beam. At a surface wave range of 200 km, the minimum detectable radar cross sections vary between 18 and 30 dBm^2 (daytime) and 30 and 42 dBm^2 (nighttime), as the wind direction varies from parallel to the radar beam to perpendicular. The minimum cross section also varies with the first power of range. During periods of spread F ionospheric turbulence the minimum detectable vessel RCS may increase by 20 dB.

Résumé

Le document présente et analyse une configuration de radar haute fréquence comprenant un trajet d'émission d'ondes ionosphériques et un trajet de réception d'ondes de surface. Les limites de résolution du radar sont déterminées par une formulation analytique de tracé de rayon applicable à la propagation d'un signal radar dans un plasma ionosphérique. Cette résolution est ensuite substituée dans l'équation du radar. On découvre que la détection des navires de surface à basse vitesse est limitée par le clutter océanique. Dans ce mode de détection limité par le clutter, il s'avère que la surface équivalente radar (SER) minimale observable d'un navire dépend de la direction du vent par rapport au faisceau radar. Pour une onde de surface de 200 km, la surface équivalente radar minimale observable varie entre 18 et 30 dB/m^2 (le jour) et entre 30 et 42 dB/m^2 (la nuit), alors que le vent passe d'une direction parallèle au faisceau radar à une direction perpendiculaire. La surface équivalente minimale varie aussi avec la première puissance de la distance. Durant les périodes de turbulence ionosphérique sur la couche F étalée, la SER minimale détectable d'un navire peut augmenter de 20 dB.

This page intentionally left blank.

Executive summary

Ship Detection Performance of a High Frequency Hybrid Sky-Surface Wave Radar

R. J. Riddolls; DRDC Ottawa TM 2007-327; Defence R&D Canada – Ottawa; December 2007.

A high frequency (HF) radar configuration consisting of a skywave transmit path and a surface wave receive path is presented and analyzed. The transmit signal consists of radiation from a ground-based station that is reflected from the ionosphere to illuminate targets beyond the earth's horizon. If these targets are surface vessels located within a few hundred kilometers of a shoreline, then it is feasible to place an HF receiving array on the shore to detect the scattered surface wave signal from these surface targets.

The region of ocean observable by the surface wave receiver is generally two orders of magnitude smaller in area than the ocean illuminated by the skywave transmitter. Thus it is necessary for the skywave radar transmit beam to be steered in the direction of the surface wave coverage region for long periods of time, which conflicts with the requirement for the skywave radar to scan over its coverage region. The use of multiple-input multiple-output (MIMO) transmit waveform schemes will allow arbitrary transmit beams to be formed on receive, which will mitigate this conflict.

The major limitation to the performance of the hybrid system is the broadening of the radar resolution cell that occurs during the signal propagation through the ionosphere. Irregularities in the structure of the ionospheric plasma cause the signal to lose coherence during transit, which places a lower bound on the precision of target angular and Doppler information, and to a lesser extent range information. The finite-size resolution cell will also contain radar clutter signals consisting of reflections from the surface of the ocean. These clutter signals provide the lower bound on the detectable vessel size. It is found that the minimum detectable radar cross section (RCS) of low-velocity vessels depends on the direction of the wind relative to the radar beam. At a range of 200 km, minimum detectable RCS varies between 18 and 30 dBm^2 (daytime) and 30 and 42 dBm^2 (nighttime), as the wind direction varies from parallel to the radar beam to perpendicular. This roughly corresponds to a minimum detectable vessel size of 1,000 tons during the day and 10,000 tons at night, for all wind directions. The minimum detectable vessel RCS also varies with the first power of range and inversely with the square of the one-way ionospheric correlation time, which is taken as 100 seconds. During periods of so-called spread F ionospheric turbulence, this correlation time may drop to 10 seconds, which will increase the minimum detectable target RCS by 20 dB.

Overall, the advantages of a hybrid radar system over a surface wave system are threefold. First, the hybrid radar system allows many separate surface wave receiver systems to operate without their own transmitters, mitigating the problem of spectral congestion. Second, the high power of the skywave transmitter in the hybrid system allows one to maintain clutter-limited detection at farther ranges and at higher carrier frequencies than in a surface wave-only system, which permits better detection performance at the far ranges. Third, the hybrid system avoids near-vertical incidence ionospheric clutter that is a problem with surface wave-only systems. The main drawback of the hybrid system is that the size of its resolution cell is about an order of magnitude larger than a surface wave-only system, which tends to prevent the detection of small, 30 dBm^2 (1,000 ton), vessels at night.

Sommaire

Ship Detection Performance of a High Frequency Hybrid Sky-Surface Wave Radar

R. J. Riddolls; DRDC Ottawa TM 2007-327; R & D pour la défense Canada – Ottawa; décembre 2007.

Le document présente et analyse une configuration de radar haute fréquence (HF) comprenant un trajet d'émission d'ondes ionosphériques et un trajet de réception d'ondes de surface. Le signal d'émission est constitué d'un rayonnement provenant d'une station au sol et réfléchi par l'ionosphère pour illuminer les cibles situées au-delà de l'horizon terrestre. Lorsque ces cibles sont des navires de surface situées à moins de quelques centaines de kilomètres d'une côte, il est possible d'installer une antenne réseau de réception HF sur la côte afin de détecter les ondes de surface diffusées qui proviennent de ces cibles de surface.

La région de l'océan qui est observable au moyen du récepteur d'ondes de surface est généralement deux fois plus petite que la région de l'océan qui est illuminée par l'émetteur d'ondes ionosphériques. Il est donc nécessaire que le faisceau d'émission du radar à ondes ionosphériques soit orienté dans la direction de la région de couverture par ondes de surface durant de longues périodes de temps, ce qui est incompatible avec la nécessité que le radar à ondes ionosphériques balaie sa région de couverture. Les systèmes d'émission à entrées multiples et sorties multiples (MIMO) permettent la mise en forme de faisceaux d'émission arbitraires à la réception, de manière à atténuer cette incompatibilité.

La principale limite au rendement du système hybride tient à l'élargissement de la cellule de résolution du radar durant la propagation des signaux dans l'ionosphère. En raison des irrégularités dans la structure du plasma ionosphérique, il se produit une perte de cohérence du signal durant la transmission, de sorte qu'une limite inférieure est établie pour la précision de l'information angulaire et Doppler des cibles ainsi que, dans une moindre mesure, de l'information de distance. La cellule de résolution à dimensions finies contient aussi des signaux de clutter radar provenant des réflexions à la surface de l'océan. Ces signaux de clutter déterminent la limite inférieure de la taille détectable des navires. Il s'avère que la surface équivalente radar (SER) minimale détectable d'un navire à basse vitesse dépend de la direction du vent par rapport au faisceau radar. À une distance de 200 km, la SER minimale observable varie entre 18 et 30 dB/m^2 (le jour) et entre 30 et 42 dB/m^2 (la nuit), alors que le vent passe d'une direction parallèle au faisceau radar à une direction perpendiculaire. Cette SER minimale observable est à peu près celle d'un navire de 1000 tonnes le jour et de 10 000 tonnes la nuit. La SER minimale détectable d'un navire varie aussi

avec la première puissance de la distance et inversement au carré de la durée de corrélation ionosphérique unilatérale, fixée à 100 secondes. Durant les périodes de ce qu'on appelle la turbulence ionosphérique sur la couche F étalée, cette durée de corrélation peut chuter à 10 secondes, faisant augmenter de 20 dB la SER minimale observable.

Dans l'ensemble, le système radar hybride présente trois avantages par rapport au système à ondes de surface. Premièrement, le système radar hybride permet d'utiliser plusieurs systèmes différents de réception d'ondes de surface sans leur propre émetteur, ce qui atténue le problème d'encombrement du spectre. Deuxièmement, la haute puissance de l'émetteur d'ondes ionosphériques du système hybride permet de maintenir la détection limitée par le clutter à des distances plus grandes et à des fréquences porteuses plus élevées que celles du système à ondes de surface seulement, améliorant ainsi le rendement de détection aux grandes distances. Troisièmement, le système hybride élimine le clutter ionosphérique à incidence quasi-verticale, qui pose un problème dans les systèmes à ondes de surface seulement. Le principal inconvénient du système hybride tient au fait que la taille de sa cellule de résolution est supérieure d'à peu près un ordre de grandeur à celle d'un système à ondes de surface seulement, ce qui tend à empêcher la détection des petits navires de 30 dB/m^2 (1000 tonnes) la nuit.

Table of contents

List of figures

This page intentionally left blank.

1 Introduction

Wide area surveillance depends on the ability to position sensors at high enough altitudes to see around the curvature of the earth's surface. Conventional microwave radar surveillance schemes employ airplane or satellite platforms to achieve the required altitude. HF radar systems exploit refractive and diffractive properties of HF waves to illuminate targets beyond the earth's horizon. Skywave HF radars use the ionosphere as a mirror to view distant targets. Surface wave HF radars exploit the diffraction of waves over the conducting ocean surface to illuminate targets beyond the horizon [1].

In terms of coverage area, the skywave radars provide by far the largest surveillance capability, being effective against targets out to 2,000 nautical miles (nmi) [1]. The major difficulty lies in the decorrelation of the radar signals as they propagate through the ionosphere. This decorrelation tends to place limits on the resolvability of targets, and in particular, the detectability of low-velocity ocean vessel targets in the presence of ocean clutter. Surface wave radars avoid the ionospheric path, but come with the tradeoff that the diffracted surface wave is highly attenuated, which tends to limit range to about 200 nmi [2].

As sensor technologies mature, an emerging trend is to pursue coordinated operation of multiple sensors to maximize extraction of information from the environment. In the context of HF radar, there has been interest in Canada and abroad in the performance capabilities of a hybrid sky-surface wave system, whereby waves are launched in skywave mode, but the echo propagates in surface wave mode, as shown in Figure 1. This configuration can be viewed as a sensor of opportunity, whereby the skywave radar operates without being aware of surface wave receivers that could detect echoes from ships within the region illuminated by the skywave radar.

In terms of the coverage areas cited above, the region of ocean observable by the surface wave receiver is about two orders of magnitude smaller in area than the ocean illuminated by the skywave transmitter. Thus it is necessary for the skywave radar transmit beam to be steered in the direction of the surface wave coverage region for long periods of time, which conflicts with the requirement for the skywave radar to scan its coverage region. Conversely, using the skywave transmitter as a signal of opportunity would severely limit the coherent integration times of the surface wave receiver. However, the advent of multiple-input multiple-output (MIMO) transmit waveform schemes will allow different transmit beams to be formed on receive by the surface wave and skywave operators, permitting each user to form their desired areas of target illumination [3]. MIMO will not be discussed here, but it is assumed that such a scheme will need to be employed by the skywave transmitter for the hybrid radar configuration to work.

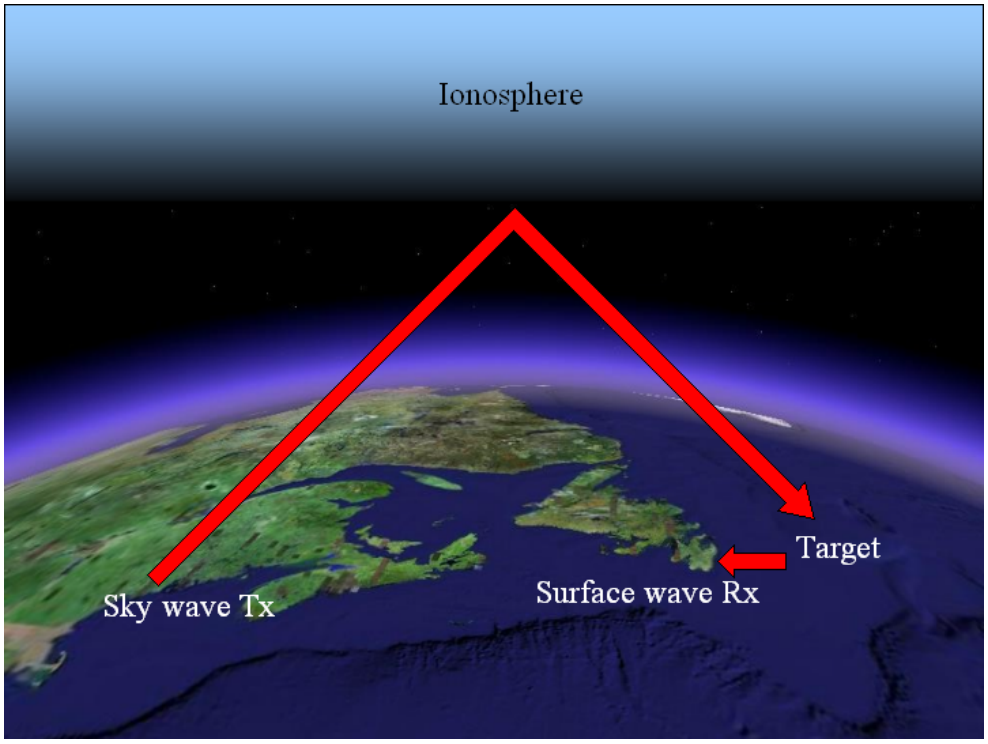

Figure 1: *Ship detection by hybrid radar.*

This report consolidates all the necessary physical concepts of a hybrid sky-surface wave radar systems and assesses the feasibility of such a concept. Chapter 2 discusses the radar range equation for the hybrid mode radar. Chapter 3 determines the fundamental limits on the ability of such a hybrid system to resolve targets. As will be shown, the resolution cell size depends largely on the HF signal environment and the coherence properties of the ionospheric propagation path. Chapter 4 will consolidate the ideas of Chapter 2 and Chapter 3 to determine the detection limits for a hybrid mode radar. The cases of both noise-limited detection and clutter-limited detection will be considered, and the minimum detectable target radar cross section (RCS) will be determined. A conclusion will be made in Chapter 5.

2 Performance equations for hybrid radar

This chapter describes the radar range equation for a hybrid radar configuration and discusses the numbers to be used in this equation.

2.1 The radar range equation

The bistatic radar range equation for coherent radar systems is given by [1]

$$\mathrm{SNR} = \frac{P_{av} G_t G_r F_t F_r \lambda^2 \sigma T_i}{(4\pi)^3 d_t^2 d_r^2 N_b}. \tag{1}$$

Here, SNR is the signal-to-noise ratio, P_{av} is the average transmit power, G_t and G_r are the transmit and receive antenna gains, F_t is the attenuation function describing losses in the medium between the transmit antenna and the target, F_r is the attenuation function describing losses in the medium between the target and the receive antenna, λ is the radar wavelength, σ is the target cross section, T_i is the coherent integration time, d_t and d_r are the distances from the target to the transmit and receive antennas, and N_b is the noise per unit bandwidth. The following sections describe the appropriate quantities to use in this equation in the calculation of target SNR.

2.2 Transmitter power

The hybrid radar configuration requires considerable transmit power to provide adequate over-the-horizon target illumination. The figure of merit for target illumination is the effective radiated power (ERP), which is equal to the transmit power times the transmit antenna gain. Most skywave radar systems run in the vicinity of about 100 MW ERP. This ERP level is achieved using about 1 MW of transmit power and about 20 dB of transmit antenna gain (see Section 2.3). Even larger ERPs, on the order of 1 GW, have been obtained for the purpose of so-called HF ionospheric heating experiments [4]. However, significant absorption of HF energy occurs in this case, as the higher power waves tend to excite a feedback loop in the bottomside ionosphere: higher wave power leads to plasma heating, which leads to increased wave attenuation, which leads to further heating, and so on. The consequence is that the radar signal becomes absorbed as a result of its own action on the ionospheric plasma. Thus, 1 MW of transmit power fed to a 20-dB gain transmit antenna can be thought of as a rough upper bound on the ERP to avoid significant self-absorption through ionospheric modification. In order to maximize the average power P_{av}, skywave radar transmitters commonly employ the 100%-duty cycle frequency modulated continuous wave (FMCW) waveform. This waveform requires the transmit and receive antennas to be separated by at least 100 km, which is easily accommodated in the hybrid radar scheme.

2.3 Transmit antenna gain

Most skywave radar systems employ transmit arrays providing gains of around 20 dB. Such an array may consist of a linear arrangement of 10 to 20 elements, where each element may be a log-periodic array of vertical monopoles. The choice of log-periodic array elements allows the operator to run the radar over a wide range of frequencies to accommodate the time-varying frequency support of the reflecting ionospheric layer. The optimal spacing of the transmit array elements is half of the radar signal wavelength. Since this requirement cannot be met over a wide range of frequencies, often two or more separate transmit arrays are used for different frequency bands of the radar [5].

The normal mode of operation of the radar transmit array is to steer a transmit beam to a particular location, dwell for a fixed coherent integration time, and then steer to a new angle. In a surveillance mode, the transmit beam must steer through the entire surveillance region before the target tracks can be updated. The required update rate for the tracks places constraints on the azimuthal width of the transmit beam and/or the coherent integration time. Furthermore, more than one carrier frequency is often required to achieve adequate target illumination throughout the coverage range of the radar. Thus, for example, a sequence of 10 transmit beam positions, 3 frequencies, with a 10-second coherent integration time, would lead to a track update time of 300 seconds.

A recent innovation in radar technology involves the use of MIMO concepts, whereby each transmit antenna element transmits a different signal selected from a set of mutually orthogonal waveforms [3]. The signal from each transmit antenna can be separated on receive using matched filtering techniques, and linearly combining the echoes from various transmit antennas effectively allows transmit beam steering on receive. The MIMO scheme allows a particular patch of the surveillance area to remain illuminated while other portions of the area are searched. This capability is critical for hybrid radar, as the surveillance area detectable by the surface wave receive array is small compared to the total surveillance area of the skywave radar. A user of the hybrid radar configuration can thus maintain surveillance coverage of their small area of interest while the user of the skywave radar maintains their larger surveillance coverage area.

2.4 Receive antenna gain

The receiving system at HF usually runs in an external noise-limited mode of operation. In this mode, noise sources external to the radar, as opposed to receiver noise, determine the lower power threshold on target detection. As long as the external noise limitation is maintained [1], receive antennas and receivers at HF need

not be impedance matched, which allows the designers to use low-cost, short vertical monopoles [2]. The low-cost factor allows one to field a large receive array. In skywave radar systems these arrays may have several hundred elements arranged in a row stretching several kilometers. Ultimately, performance limits are reached when the angular resolving power of this large receive aperture exceeds the angular width of the received signals themselves, the latter of which is discussed in Chapter 3. Thus, we will defer assigning a numerical value to the receive gain at this time.

It should, however, be noted that the external noise levels (described in Section 2.9) are usually calibrated to a matched antenna, which is also the assumption of the radar range equation. Thus, any external noise described by N_b in the radar equation has already been calibrated to include the receive antenna element factor. The gain G_r appearing in the radar equation should therefore include only the array factor of the receive array. As a simple example, a broadside array of M elements at half-wavelength spacing has an array factor of M.

2.5 Transmit propagation attenuation

The transmitted signal suffers degradation while propagating through the ionosphere. Chapter 3 quantifies the loss of coherence of the signal in some detail, so in this section we will limit the discussion to changes in signal power. The power losses can arise from electron thermalization and signal depolarization [1].

Power loss in a radar signal can arise from the acceleration of ionized electrons in the ionospheric plasma by the electric field of the signal. These accelerated electrons then scatter from neutral atoms in the lower ionosphere or ionized atoms in the upper ionosphere. The scattering converts electrons with a coherently oscillating velocity to electrons with an isotropic velocity distribution (i.e. heat), which serves to damp the radar signal. This effect can usually be mitigated by proper frequency selection for the radar. This selection usually involves the skywave radar operator sending out a swept-frequency test signal, and then measuring the amplitude of ground clutter in the illuminated patch on the earth's surface as a function of frequency and group delay. The selected frequency is typically in the vicinity of 20 MHz during daytime, and in the vicinity of 7 MHz during nighttime, but with a somewhat considerable day-to-day variability [1].

The effect of depolarization is more difficult to control. A homogeneous magnetized plasma normally supports two propagation modes, as described by the cold-plasma dispersion relation [6]. The two modes are referred to as the ordinary (O) and extraordinary (X) modes. The modes are elliptically polarized, with opposite directions of electric field vector rotation. A launched linearly polarized wave therefore has similar levels of O and X mode content. However, the phase speeds of the two modes differ in the ionosphere, leading to a rotation of the linearly polarized wave during

propagation through the ionosphere, referred to as Faraday rotation. If the level of rotation is large and randomly distributed, the signal incident on the target will on average have approximately equal horizontal- and vertical-polarized components. When this signal approaches the ship target, the horizontal component of the signal is essentially shorted out by the conducting ocean surface, and does not play a part in the signal scattering or the propagation along the earth to the receiving antenna. Thus typically one might lose half the radar power through depolarization.

2.6 Receive propagation attenuation

The consideration of diffraction due to the curved Earth surface can be handled in combination with the loss due to surface conductivity. The theory of diffraction of vertically polarized waves over a lossy spherical conductor was treated in [7]. If the signal amplitude transmitted over a perfectly conducting flat ground plane is 1, then the additional effect of finite conductivity and surface curvature would introduce an attenuation factor of [7]

$$F = \exp\{j[k_0(r-d) - \pi/4]\}\frac{(\pi x)^{1/2}}{2}\sum_{s=1}^{\infty}\frac{\exp(-jxt_s)}{t_s - q^2}, \tag{2}$$

where r is the straight-line distance between the transmitter and receiver, d is the arc length along the earth's surface, x and q are given by

$$x = da^{-2/3}(k_0/2)^{1/3} \tag{3}$$

$$q = -j(k_0 a/2)^{1/3}(1/n)[1-(1/n)^2]^{1/2}, \tag{4}$$

where a is the radius of the earth, k_0 is the radar wavenumber, n is the index of refraction of the surface, and t_s is the sth root of

$$w'(t) - qw(t) = 0, \tag{5}$$

where $w(t)$ is defined by [7]

$$w(t) = 2\sqrt{\pi}\exp(-j\pi/6)\mathrm{Ai}[t\exp(-j2\pi/3)]. \tag{6}$$

The Airy function $\mathrm{Ai}(t)$ is defined as the solution to the differential equation

$$w''(t) - tw(t) = 0. \tag{7}$$

Plots of the attenuation factor F as a function of distance are shown in Figure 2.

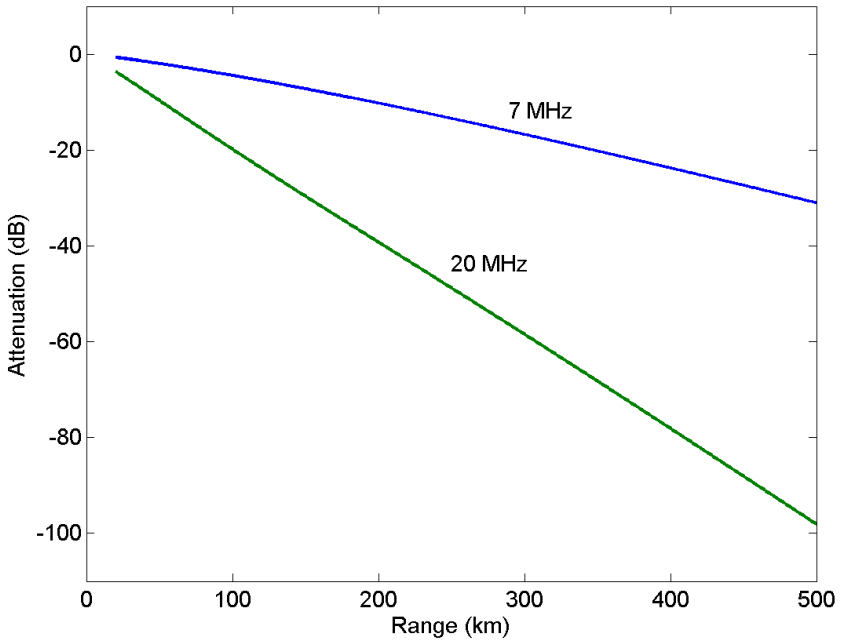

Figure 2: *One-way signal attenuation for surface wave propagation.*

2.7 Target radar cross section

The ship target rests on a ground plane, and therefore one must consider the effect of this ground plane on the scattering problem. A total of three reflections from the ground plane occur, as shown in Figure 3. The first reflection occurs in the vicinity of the transmit antenna. This is accounted for by the usual calculation of the gain of an antenna operating over a ground plane. This calculation assumes a doubling of the radiated electric field, or equivalently the quadrupling of the radiated power. For example, a quarter-wave monopole would have a gain G_t equal to +5.15 dBi [8].

Two more reflections occur in the vicinity of the ship. These effects are lumped into the cross section calculation of the ship. Namely, we place a ship on a ground plane and aim an electric field E_i at the ship from a finite elevation angle, such that the total field incident on the ship after the ingoing ground plane reflection is $2E_i$. This leads to a scattered electric field $E_s/2$, such that the total radiated field after the outgoing ground plane reflection is E_s. The ship cross section is $4\pi R^2 E_s^2/E_i^2$, where R is the distance from the ship at which the scattered electric fields are measured.

Note that because of the geometry, a fourth reflection does not occur in the vicinity of the receive surface wave antenna. Thus, one cannot use the normal gain of an antenna over a ground plane, where a reflection is assumed. One has to remove the

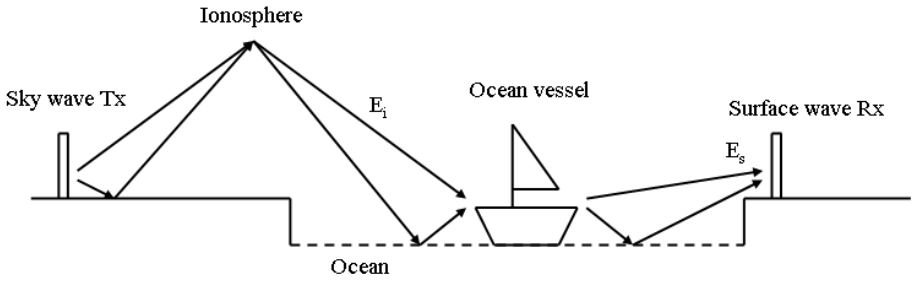

Figure 3: *Effect of ground plane.*

quadrupling of the flux (or 6 dB) from any such calculation, such that the gain of a quarter-wave monopole is -0.85 dBi [8].

2.8 Coherent integration time

As discussed under the topic of transmit antenna gain above, the coherent integration time is constrained by the duration of time for which the radar operator steers a transmit beam to a particular patch of the surveillance region. In normal skywave radar surveillance operation, this time is limited by the requirement for the tracker to update target track information throughout the entire surveillance region, and is normally limited to about 10 seconds. With the advent of MIMO transmitters, the entire surveillance region can be simultaneously illuminated, which would allow for longer integration times [3].

Skywave radars may operate with bandwidths of approximately 10 kHz, which provides a radar resolution cell depth of about 15 km. A ship travelling at 10 knots radial velocity would stay within such a resolution cell for nearly an hour. However, the ionospheric signals in a one-way pass through the ionosphere typically do not maintain coherence for more than 100 seconds during good conditions, and perhaps 10 seconds during conditions of elevated ionospheric turbulence, which places a hard limit on the usable integration time. The ionospheric coherence time can easily be measured by a one-way skywave signal link, and is further discussed in Chapter 3.

2.9 Noise density

Plots of environmental noise power spectral density have been published by the International Telecommunication Union (ITU) [9]. The lower limit of radio noise is due to worldwide lightning activity. Since most lightning activity is concentrated in the tropics, radio noise tends to lessen towards the earth's poles. Man-made radio

noise due to air ionization by electrical arcs in motors, welders, spark plugs, and so on, causes additional noise contributions that often dominate the atmospheric background. The man-made contributions have been classified by the ITU as business, residential, rural, and quiet rural, in order of decreasing noise level. Obviously, quiet rural sites are preferable for radar operation, and normally noise levels are a basis for site selection. The quiet rural noise level is [9]

$$N_b = 9.2 \times 10^{-16} f^{-2.86}, \tag{8}$$

in units of W/Hz, where f is in MHz. Furthermore, above 10 MHz galactic noise can penetrate the ionosphere and becomes the dominant noise source. It is given by [9]

$$N_b = 6.3 \times 10^{-16} f^{-2.30}, \tag{9}$$

with the same units as the previous equation.

3 Resolution limits of hybrid mode radar

In this section, we determine the resolution limits imposed by the skywave transmission path through the ionosphere. The formulation is based on an analytic theory of ray tracing.

A radar pulse propagates through the ionosphere according to a dispersion relation that relates the pulse location $\mathbf{r}$, group delay t, wavenumber $\mathbf{k}$, and frequency ω, and can be written as an implicit function $G(\mathbf{r}, t, \mathbf{k}, \omega) = 0$. The evolution of $(\mathbf{r}, t, \mathbf{k}, \omega)$ during propagation is described by ray tracing equations [6]:

$$\frac{d\mathbf{r}}{d\tau} = \frac{\partial G}{\partial \mathbf{k}} \qquad \frac{dt}{d\tau} = -\frac{\partial G}{\partial \omega} \qquad \frac{d\mathbf{k}}{d\tau} = -\frac{\partial G}{\partial \mathbf{r}} \qquad \frac{d\omega}{d\tau} = \frac{\partial G}{\partial t}, \tag{10}$$

where τ parameterizes the trajectory of the pulse in $(\mathbf{r}, t, \mathbf{k}, \omega)$-space referred to as the "ray" or "ray path". A more explicit form of the ray tracing equations can be achieved by assuming that the medium is plane-stratified, such that the dispersion relation $G = 0$ has spatial variation that depends on altitude z only, making it possible to write the ray tracing equations as derivatives with respect to the altitude co-ordinate. For example, the first ray tracing equation becomes:

$$\frac{d\mathbf{r}}{dz} = \frac{d\mathbf{r}/d\tau}{dz/d\tau} = \frac{\partial G/\partial \mathbf{k}}{\partial G/\partial k_z} = -\frac{\partial k_z}{\partial \mathbf{k}}, \tag{11}$$

where k_z is the z component of $\mathbf{k}$. If we view the ionosphere as a continuum of layers, then an application of Snell's law at the boundary of each layer implies that the horizontal wavenumbers k_x and k_y are conserved during propagation. Thus $\partial k_z/\partial \mathbf{k}$ is well-defined and Equation (11) can be integrated easily. This formulation permits very general expressions for k_z, such as the Booker quartic [10].

3.1 Path integral formulation of radar pulse properties

We now consider the effects of ionospheric plasma irregularities on the propagation of a radar pulse. Irregularities are density structures in the ionospheric plasma that are small compared to the scale size of the overall ionosphere. The problem of propagation in irregularities was first solved for isotropic media [11], and was later applied to the problem of phase scintillation of VHF and microwave signals [12]. Recently, the isotropic theory has found application in the description of the Doppler spreading of HF skywave radar signals [13], which we further refine here to allow for anisotropic refractive index and wavenumber spreading (also see [14]). Although the theory can also be used for spreading in radar pulse position $\mathbf{r}$ and group delay t, spreading in these co-ordinates is not always observed at HF due to the limited range resolution of HF radar systems. Thus, discussion of range resolution will be deferred.

We integrate the two ray tracing equations relevant to azimuth ($\mathbf{k}$) and Doppler (ω) under the assumption of plane-stratification to arrive at the change in these quantities following propagation in the ionosphere:

$$\Delta\mathbf{k} = \int dz\, \frac{\partial k_z}{\partial \mathbf{r}} \qquad \Delta\omega = -\int dz\, \frac{\partial k_z}{\partial t}. \tag{12}$$

We now perturb k_z to account for the presence of ionospheric plasma density irregularities. We denote the background plasma density as N_0 and the irregularity density as N_1, such that the total plasma density is $N = N_0 + N_1$, where N_1 has zero mean. The perturbed wavenumber to first order in N_1 is

$$k_z(N) = k_z(N_0) + N_1 \left.\frac{\partial k_z}{\partial N}\right|_{N_0}. \tag{13}$$

If the spatial variation in N_0 is slow compared to that of N_1, and N_0 does not vary in time, then we find that to first order:

$$\Delta\mathbf{k} = \int dz\, \frac{\partial N_1}{\partial \mathbf{r}} \frac{\partial k_z}{\partial N} \qquad \Delta\omega = -\int dz\, \frac{\partial N_1}{\partial t} \frac{\partial k_z}{\partial N}. \tag{14}$$

Thus $\Delta\mathbf{k}$ and $\Delta\omega$ can be expressed as linear combinations of the zero-mean random variables $\partial N_1/\partial \mathbf{r}$ and $\partial N_1/\partial t$. The integrals above are equivalent to a summation over many uncorrelated random variables, and so the spectra of the sums is equal to the sums of the spectra of the variables, or more precisely,

$$\begin{aligned} S_{\Delta\mathbf{k}}(\kappa_x, \kappa_y, \Omega) &= \int dz \left(\frac{\partial k_z}{\partial N}\right)^2 S_{\frac{\partial N}{\partial \mathbf{r}}}(\kappa_x, \kappa_y, \kappa_z = 0, \Omega) \\ S_{\Delta\omega}(\kappa_x, \kappa_y, \Omega) &= \int dz \left(\frac{\partial k_z}{\partial N}\right)^2 S_{\frac{\partial N_1}{\partial t}}(\kappa_x, \kappa_y, \kappa_z = 0, \Omega). \end{aligned} \tag{15}$$

To avoid possible confusion, the notations κ and Ω are used to denote wavenumbers and frequencies parameterizing the spectra of $\Delta\mathbf{k}$ and $\Delta\omega$. Now, by a property of Fourier transforms, we have that

$$S_{\frac{\partial N_1}{\partial x}} = \kappa_x^2 S_{N_1} \qquad S_{\frac{\partial N_1}{\partial y}} = \kappa_y^2 S_{N_1} \qquad S_{\frac{\partial N_1}{\partial t}} = \Omega^2 S_{N_1}. \tag{16}$$

However, the frequency and wavenumbers are related to the signal phase ϕ by

$$\Delta k_x = \frac{\partial \phi}{\partial x} \qquad \Delta k_y = \frac{\partial \phi}{\partial y} \qquad \Delta\omega = \frac{\partial \phi}{\partial t}, \tag{17}$$

so that we have that the $\Delta\mathbf{k}$ and $\Delta\omega$ spectra are related to the phase spectrum by

$$S_{\Delta k_x} = \kappa_x^2 S_\phi \qquad S_{\Delta k_y} = \kappa_y^2 S_\phi \qquad S_{\Delta\omega} = \Omega^2 S_\phi. \tag{18}$$

Combining the above equations, we conclude that the spectrum of the phase is given by

$$S_\phi(\kappa_x, \kappa_y, \Omega) = \int dz \left(\frac{\partial k_z}{\partial N}\right)^2 S_{N_1}(\kappa_x, \kappa_y, \kappa_z = 0, \Omega). \tag{19}$$

As for S_{N_1} itself, we use a spectrum model for plasma irregularities that follows a 4th-order power law [15], and a dispersion relation for near-perpendicular drift wave turbulence [16]:

$$S_{N_1}(\boldsymbol{\kappa}, \Omega) = \frac{4\sqrt{2\alpha}\pi^2 E[N_1^2(z)]\kappa_0^{-3}}{1 + \kappa_0^{-4}(\kappa_\perp^2 + \alpha\kappa_\parallel^2)^2}\delta(|\Omega| - \kappa_\perp v_d). \tag{20}$$

Here, v_d is the diamagnetic drift velocity (≤ 60 m/s), κ_0 is the outer scale length ($\approx 10^{-4}$ m^{-1}), α is an anisotropy factor (≈ 3000), $\kappa_\perp$ is the magnitude of the component of the density irregularity wavenumber $\boldsymbol{\kappa}$ that is perpendicular to the earth's magnetic field, $\kappa_\parallel$ is the magnitude of the component of $\boldsymbol{\kappa}$ along the field, and the variance of the density fluctuations $E[N_1^2(z)]$ is assumed to be a function of altitude z. We suppose the magnetic field of the earth follows a unit vector $\hat{\mathbf{l}} = (l_x, l_y, l_z)$. Quantities $\kappa_\parallel$ and $\kappa_\perp$ are:

$$\kappa_\parallel = \boldsymbol{\kappa} \cdot \hat{\mathbf{l}} \qquad \kappa_\perp = ||\boldsymbol{\kappa} - \kappa_\parallel \hat{\mathbf{l}}||. \tag{21}$$

Although z is constrained to be vertical, at this point we can rotate x and y azimuthally without loss of generality such that the magnetic field vector lies in the y-z plane and $l_x = 0$. Therefore we conclude that

$$S_\phi(\kappa_x, \kappa_y, \Omega) = \frac{4\sqrt{2\alpha}\pi^2\kappa_0^{-3}\delta[|\Omega| - (\kappa_x^2 + l_z^2\kappa_y^2)^{1/2}v_d]}{1 + \kappa_0^{-4}[\kappa_x^2 + (l_z^2 + \alpha l_y^2)\kappa_y^2]^2} \int dz\, E[N_1^2(z)] \left(\frac{\partial k_z}{\partial N}\right)^2. \tag{22}$$

3.2 Spatial and temporal correlation

We seek the spread in $\mathbf{k}$ and ω arising from processing radar signals with this phase spectrum. On the basis of $\alpha \gg 1$, we assume that the spectrum is negligible when $\kappa_x \approx \kappa_y$. This allows the form of the delta function and the denominator to be simplified. For now, we also ignore the scalar amplitude of the spectrum for simplicity. Thus,

$$S_\phi(\kappa_x, \kappa_y, \Omega) \propto \frac{\delta(|\Omega| - |\kappa_x|v_d)}{1 + \kappa_0^{-4}(\kappa_x^2 + \alpha l_y^2\kappa_y^2)^2}. \tag{23}$$

The space-time autocorrelation of the phase is given by the inverse Fourier transform:

$$R_\phi(X, Y, T) \propto \iiint d\kappa_x d\kappa_y d\Omega\ S_\phi\, e^{i\kappa_x X + i\kappa_y Y - i\Omega T} \tag{24}$$

$$\propto \iint d\kappa_x d\kappa_y \frac{e^{i\kappa_x X + i\kappa_y Y'}(e^{i\kappa_x v_d T} + e^{-i\kappa_x v_d T})}{1 + \kappa_0^{-4}(\kappa_x^2 + \kappa_y^2)^2}, \tag{25}$$

where $Y' = Y/(\sqrt{\alpha} l_y)$. Going to polar co-ordinates and integrating over azimuth, we find that

$$R_\phi(X,Y,T) \propto \sum_{m=1,-1} \int_0^\infty du\, \frac{u J_0(u\kappa_0 \sqrt{(X+mv_dT)^2 + Y'^2})}{1+u^4}$$
$$\propto \sum_{m=1,-1} \int_{-\infty}^\infty du\, \frac{u H_0^{(1)}(u\kappa_0 \sqrt{(X+mv_dT)^2 + Y'^2})}{1+u^4}. \quad (26)$$

To evaluate the integral, we form a closed contour in the upper half plane enclosing the poles at $e^{i\pi/4}$ and $e^{3i\pi/4}$. Using the residue theorem, we find that

$$R_\phi(X,Y,Z) \propto \sum_{m=1,-1} \mathrm{kei}(\kappa_0 \sqrt{(X+mv_dT)^2 + Y'^2}), \quad (27)$$

where kei is a Kelvin function, defined as

$$\mathrm{ker}(x) + i\mathrm{kei}(x) = \frac{\pi i}{2} H_0^{(1)}(x e^{3\pi i/4}). \quad (28)$$

The autocorrelation at zero lag is simply the mean-square phase fluctuation $E(\phi^2)$. Since $\mathrm{kei}(0) = -\pi/4$, we can write

$$R_\phi(X,Y,T) = -\frac{2}{\pi} E(\phi^2) \sum_{m=1,-1} \mathrm{kei}(\kappa_0 \sqrt{(X+mv_dT)^2 + Y'^2}). \quad (29)$$

The central limit theorem implies Gaussian single-point statistics for ϕ. Thus, we can relate R_ϕ to the autocorrelation of the complex signal amplitude $A = e^{i\phi}$ using [17]:

$$E\left[e^{-i\phi(x,y,t)} e^{i\phi(x+X,y+Y,t+T)}\right] = e^{R_\phi(X,Y,T) - E(\phi^2)}. \quad (30)$$

The complex amplitude autocorrelation function is therefore

$$R_A(X,Y,T) = e^{-E(\phi^2)\left[1 + \frac{2}{\pi}\sum_{m=\pm 1} \mathrm{kei}(\kappa_0 \sqrt{(X+mv_dT)^2 + Y'^2})\right]}. \quad (31)$$

This expression provides the space-time correlation distance, which will be used in Chapter 4 to determine the radar resolution cell size. However, we will note here that the horizontal correlation distance observed on the ground is at very best on the order of a couple kilometers. This limited correlation distance precludes signal processing schemes whereby the direct transmitter-receiver ionospheric reflection signal is used to correct for resolution degradation in the hybrid radar target signal.

4 Ship detectability

The objective of this chapter is to determine the minimum RCS of a ship that is detectable. The method used will depend on whether the detection of the ship is limited by clutter or limited by external noise. The first task is therefore to compute the clutter level produced by the ocean. This is done in Section 4.1. The second task is to determine whether detection is clutter or noise limited. Section 4.2 will prove that the detection is clutter-limited over all ranges of interest. Section 4.3 then determines the minimum detectable RCS of ships.

4.1 The sea clutter cross section

Expressions for the HF radar cross section $\sigma(\omega)$ of the ocean per m^2 ocean surface area per rad/s bandwidth have been presented [8, 18] and have been used for ship visibility calculations for particular skywave radar systems [19] (also see [20] for some experimental results). We assume that the incident signal on the patch of ocean is at low elevation (<20 degrees), and for simplicity take the surface wave radar to be more or less on a line connecting the target and skywave radar, as depicted in Figure 1. Under these assumptions, the scattering is of the backscatter type, and the cross section per unit area, per unit Doppler frequency, is given by [18]

$$\sigma(\omega) = \sigma_1(\omega) + \sigma_2(\omega) \tag{32}$$

$$\sigma_1(\omega) = 2^6 \pi k_0^4 \sum_{m=\pm 1} S(-2m\mathbf{k}_0)\delta(\omega - m\omega_B) \tag{33}$$

$$\sigma_2(\omega) = 2^6 \pi k_0^4 \sum_{m,m'=\pm 1} \iint dp\, dq\, |\Gamma|^2 S(m\mathbf{k}) S(m'\mathbf{k}')\delta(\omega - m\sqrt{gk} - m'\sqrt{gk'}). \tag{34}$$

Here, σ_1 is the so-called first-order backscatter RCS that consists of "Bragg lines" at discrete positive and negative Doppler frequencies $\omega_B = \sqrt{2gk_0}$, where g is the gravitational acceleration of 9.8 $\mathrm{m/s}^2$, and k_0 is the radar wavenumber. σ_2 is the second-order backscatter, which occupies a continuum of Doppler frequencies. Since the visibility of ships near the Bragg lines can be mitigated by dual-frequency operation [21], we will concern ourselves here primarily with the second-order clutter continuum. In these expressions, S is the wavenumber spectrum of water waves, given by

$$S(\mathbf{k}) = f(k)g(\theta) \tag{35}$$

$$f(k) = 0.005/k^4 \quad (\text{for } k > g/v^2, \text{ zero otherwise}) \tag{36}$$

$$g(\theta) = \frac{\cos^s[(\theta - \theta^*)/2]}{\int_{-\pi}^{\pi} \cos^s(\theta/2)\, d\theta} \quad (s = 4 \text{ typically}), \tag{37}$$

where k and θ is magnitude and azimuth of $\mathbf{k}$, v is the wind speed, θ^* is the wind direction, and s is the ocean-wave spreading factor. Here, f is the nondirectional distribution, and g is the directional factor. Hence, $S(\mathbf{k})$, being a product of f and g, is a directional wavenumber spectrum.

The expression for σ_2 can be interpreted as a double scattering within a small region of ocean surface compared to the radar resolution cell. The two scattering locations within the patch are connected by a wavenumber (p, q). Following the Bragg scattering condition, the difference between the wavenumber (p, q) and the incident radar wavenumber $\mathbf{k}_0 = k_0\hat{\mathbf{x}}$ is the ocean wavenumber

$$\mathbf{k} = (p - k_0)\hat{\mathbf{x}} + q\hat{\mathbf{y}}, \tag{38}$$

producing the first scatter, and the difference between the scattered radar wavenumber $-\mathbf{k_0}$ and (p, q) is the ocean wavenumber

$$\mathbf{k}' = -(p + k_0)\hat{\mathbf{x}} - q\hat{\mathbf{y}}, \tag{39}$$

producing the second scatter. Finally, the so-called coupling coefficient Γ describes the strength of the second-order interaction, and consists of hydrodynamic (H) and electromagnetic (E) contributions [18]:

$$\Gamma = \Gamma_H + \Gamma_E \tag{40}$$

$$\Gamma_H = -\frac{i}{2}\left[k + k' - \frac{(kk' - \mathbf{k}\cdot\mathbf{k}')(\omega^2 + \omega_B^2)}{mm'\sqrt{kk'}(\omega^2 - \omega_B^2)}\right] \tag{41}$$

$$\Gamma_E = +\frac{1}{2}\left[\frac{(\mathbf{k}\cdot\mathbf{k}_0)(\mathbf{k}'\cdot\mathbf{k}_0)/k_0^2 - 2\mathbf{k}\cdot\mathbf{k}'}{\mathbf{k}\cdot\mathbf{k}' + k_0\Delta}\right] \tag{42}$$

$$\Delta = 0.011 - 0.012i \text{ m}^{-1}. \tag{43}$$

There are four free parameters in the above model: ω, f_0, v, and θ^*. To reduce the dimensions of the parameter space for ocean clutter, we consider low-Doppler ($\omega \ll \omega_B$) targets only, which compete with clutter near $\omega = 0$. In this case, it can be shown that the cross section is dominated by $\sigma_2(\omega)$, and consists of contributions from $m = -m' = 1$ only, or equivalently $m = -m' = -1$ only (see [18]). In this case, we have

$$\begin{aligned}\sigma(0) =& 2^6\pi k_0^4 \iint dp\, dq |\Gamma|^2 S(\mathbf{k})S(-\mathbf{k}')\delta(\sqrt{gk} - \sqrt{gk'}) \\ =& \frac{2^6\pi k_0^3}{\sqrt{g}} \int dq\, |\Gamma|^2 S(\mathbf{k})S(-\mathbf{k}')(k_0^2 + q^2)^{3/4}.\end{aligned} \tag{44}$$

If the wind speed is large enough such that $k_0 > g/v^2$, which is common above 6 MHz, then S is nonzero for all q, and $\sigma(0)$ is independent of v. $\sigma(0)$ thus depends on

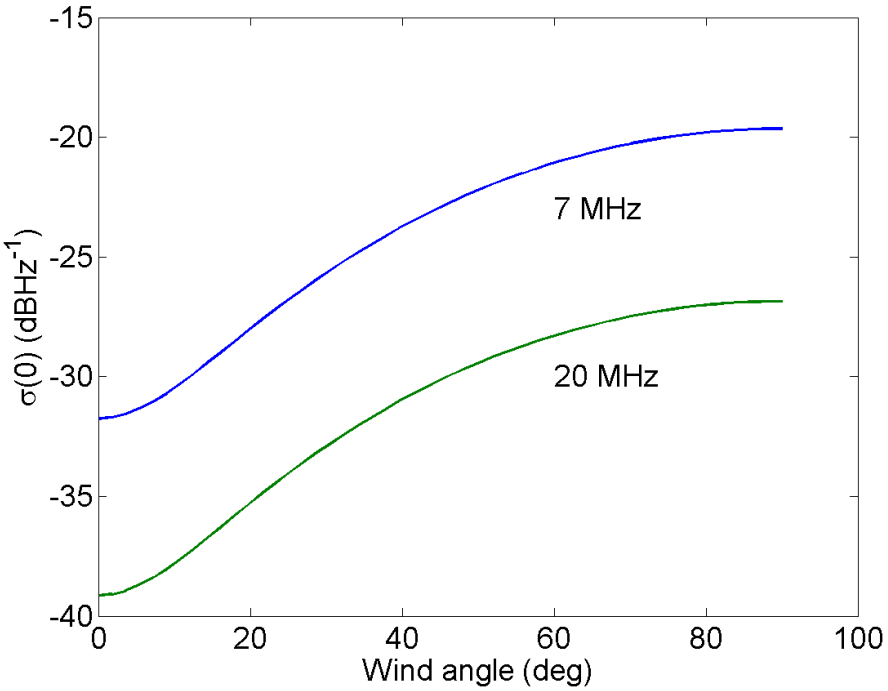

Figure 4: *RCS of ocean for various wind angles with respect to radar beam.*

f_0 and θ^* only, and is plotted in Figure 4 for typical daytime (20 MHz) and nighttime (7 MHz) HF skywave radar operating frequencies. As an average over wind angles for the next section, we will take the ocean RCS per unit area and frequency to be -33 dBm^2 in the daytime 20 MHz case and -26 dBm^2 in the nighttime 7 MHz case.

4.2 Boundary between clutter and noise-limited cases

Having computed an ocean RCS, we now seek to determine the boundary between the clutter and noise-limited cases. This boundary occurs where the radar equation predicts 0 dB SNR when observing sea clutter. To provide such a comparison, we need an expression for the total RCS within the radar resolution cell, as opposed to the RCS per unit area and frequency. The total cross section σ of the ocean in the resolution cell is given by $\sigma(0)$ times the size of the resolution cell:

$$\sigma = \sigma(0)\,\Delta r\,\Delta\omega\,d_r\Delta\psi, \tag{45}$$

where Δr is the range resolution, $\Delta\omega$ is the Doppler resolution, d_r is the target distance from the surface wave radar, and $\Delta\psi$ is the angular resolution.

The range resolution is given by the inverse of the radar bandwidth:

$$\Delta r = \frac{c}{2B}, \tag{46}$$

where c is the speed of light and B is the radar bandwidth. Δr has not been discussed so far under the premise that it is set by HF spectral occupancy. All HF radar systems run on a non-interference basis to allocated services, and thus must transmit in unused frequency channels that lie between active channels assigned to allocated services. The probability of locating and maintaining an unused channel decreases with increasing channel bandwidth. Thus, most HF skywave radars with real-time spectrum monitoring tend to operate with narrow bandwidths, usually not exceeding 10 kHz, which imposes a range resolution of about 15 km. It is assumed here that $\Delta r = 15$ km generally exceeds the group delay fluctuations that would result from an irregular ionosphere.

Equation (31) evaluated at $(X, Y) = 0$ is the temporal autocorrelation of the radar signal. This function decays to one half of its initial value in a time $T_{1/2} \leq 100$ s. This $T_{1/2}$ is the "correlation time" corresponding to one ionospheric transit, and is twice the two-way ionospheric transit correlation times discussed in the literature ([19] and others cite a maximum correlation time of 50 s). The Doppler resolution $\Delta\omega$ is the 3-dB width of the Fourier transform of the temporal autocorrelation function. Near $T_{1/2} \approx 100$ s, it is

$$\Delta\omega \approx 2\sqrt{E(\phi^2)}\kappa_0 v_d \approx 2/T_{1/2}. \tag{47}$$

$d_r\Delta\psi$ is the tangential extent of the resolution cell. It is related to the radar wavenumber k_0 and wavenumber fluctuation tangential to the radar beam Δk:

$$d_r\Delta\psi = d_r\Delta k/k_0. \tag{48}$$

The Fourier transform of Equation (31) at $(Y, T) = 0$ gives a bound on the angular resolution for all look angles:

$$\Delta k \approx 2\sqrt{E(\phi^2)}\kappa_0 \approx 2/(v_d T_{1/2}). \tag{49}$$

Combining the above equations, the ocean radar cross section is

$$\sigma = \frac{2d_r c\sigma(0)}{Bk_0 v_d T_{1/2}^2} \approx 5 \times 10^{14} \frac{d_r\sigma(0)}{Bf_0 T_{1/2}^2}. \tag{50}$$

Now that we have an expression for the cross section, we substitute into the radar range equation and equate to one. This results in the somewhat unwiedly expression:

$$\frac{F_r}{d_r} = \frac{32\pi^3 Bk_0 v_d T_{1/2}^2 d_t^2 N_b}{P_{av} G_t G_r F_t \lambda^2 c\sigma(0) T_i}. \tag{51}$$

Here, we have grouped the parameters that depend on receiver range on the left. The transmitter range is not included because its dependence on the receiver range is weak.

We assume a choice of coherent integration time equal to the maximum supported by the ionosphere $T_i \approx T_{1/2}$, and take the maximum realizable receive gain versus external noise to be $2\pi/(\Delta\psi) \approx \pi k_0 v_d T_{1/2}$. With these choices, we have

$$\frac{F_r}{d_r} = \frac{32\pi^2 B d_t^2 N_b}{P_{av} G_t F_t \lambda^2 c \sigma(0)}. \tag{52}$$

Per previous discussion, we take the following numerical values: $B \approx 10$ kHz, $P_{av}G_t \approx 10^8$ W, $F_t \approx 0.5$, and $c = 3 \times 10^8$ m/s. We assume mid-range values of the skywave transmit coverage region, where $d_t \approx 2,000$ km. We also take the following diurnal varying parameters: $N_b = 6.4 \times 10^{-19}$ W/Hz (day), $N_b = 3.5 \times 10^{-18}$ W/Hz (night), $\lambda = 15$ m (day), $\lambda = 43$ m (night), $\sigma(0) = 5.0 \times 10^{-4}$ Hz^{-1} (day), and $\sigma(0) = 2.5 \times 10^{-3}$ Hz^{-1} (night). Then we have

$$\frac{F_r}{d_r} = 4.8 \times 10^{-15} \text{ (day)} \tag{53}$$

$$= 6.4 \times 10^{-16} \text{ (night)}. \tag{54}$$

The reader can convince themselves from Figure 2 that the detection will be clutter limited out to 400 km during day or night.

4.3 Minimum detectable ship size

The clutter-limited detection mode permits straightforward evaluation of ship detection capability. One simply requires the ship cross section to exceed the clutter cross section by a detection threshold, say 10 dB. From Equation (50), we find that the minimum detectable ship RCS is given by

$$\sigma_{min} = 5 \times 10^{15} \frac{d_r \sigma(0)}{B f_0 T_{1/2}^2}. \tag{55}$$

From Figure 4, the value of $\sigma(0)$ ranges between -39 to -27 dBHz^{-1} during the day and -32 to -20 dBHz^{-1} at night. Taking other typical values $B = 10$ kHz, $f_0 = 20$ MHz (day), $f_0 = 7$ MHz (night), a value of $d_r = 200$ km for mid-range HFSWR operation, and $T_{1/2} = 100$ s for one-way ionospheric propagation, we find that

$$\sigma_{min} = 18 \text{ dBm}^2 \text{ (day, head/tailwind)} \tag{56}$$

$$= 30 \text{ dBm}^2 \text{ (day, crosswind)} \tag{57}$$

$$= 30 \text{ dBm}^2 \text{ (night, head/tailwind)} \tag{58}$$

$$= 42 \text{ dBm}^2 \text{ (night, crosswind)}. \tag{59}$$

During periods of spread F ionospheric turbulence, where the temporal correlation time may decrease by an order of magnitude, the minimum detectable vessel RCS may increase by 20 dB.

5 Conclusion

This memorandum has analyzed a hybrid sky-surface wave radar concept and made calculations of minimum detectable vessel RCS. Minimum detectable vessel RCS varies directly with range and inversely with the square of the ionospheric channel correlation time. Minimum detectable vessel RCS values also depend on day/night condition and wind direction, with daytime and head/tail winds providing better detection conditions than nighttime and cross winds.

At a surface range of 200 km, and with a one-way ionospheric correlation time of 100 s, the minimum detectable vessel RCS varies between 18 and 30 dBm^2 (daytime) and 30 and 42 dBm^2 (nighttime), as the wind direction varies from parallel to the radar beam to perpendicular. This roughly corresponds to a minimum detectable vessel size of 1,000 tons during the day and 10,000 tons at night, for all wind directions. The calculated RCS values also assume that the speed of the vessel is sufficiently slow so that its Doppler frequency lies near the center of the second-order ocean clutter continuum between the Bragg lines in the ocean echo Doppler spectrum. This assumption removes the dependence of the clutter level on wind speed.

The ocean clutter levels are proportional to the size of the radar resolution cell, which is in turn governed by the decorrelation of the signal as it propagates through the ionosphere. The correlation functions are derived from an analytic ray tracing theory that assumes a fourth-order power-law shape for the ionospheric plasma density fluctuation. This formulation allows the resolution cell volume to be recast as a function of the one-way ionospheric correlation time, which is a parameter that is easily measured and/or monitored by a low-power HF skywave communications link.

Overall, the advantages of a hybrid radar system over a surface wave system are threefold. First, the hybrid radar system allows many separate surface wave receiver systems to operate without their own transmitters, mitigating the problem of spectral congestion. Second, the high power of the skywave transmitter in the hybrid system allows one to maintain clutter-limited detection at farther ranges and at higher carrier frequencies than in a surface wave-only system, which permits better detection performance at the far ranges. Third, the hybrid system avoids near-vertical incidence ionospheric clutter that is a problem with surface wave-only systems. The main drawback of the hybrid system is that the size of its resolution cell is about an order of magnitude larger than a surface wave-only system, which tends to prevent the detection of small, 30 dBm^2 (1,000 ton), vessels at night.

References

[1] Headrick, J. M. (1990). HF over-the-horizon radar. In M. I. Skolnik, (Ed.), *Radar Handbook*, pp. 24.1–24.43. New York: McGraw-Hill.

[2] Sevgi, L., Ponsford, A. M., Chan, H. C. (2001). An integrated maritime surveillance system based on high-frequency surface-wave radars, part 1: theoretical background and numerical simulations. *IEEE Antennas and Propagation Magazine*, 43 (4), 28–43.

[3] Frazer, G. J., Abramovich, Y. I., Johnson, B. A. (2007). Spatially waveform diverse radar: perspectives for high frequency OTHR. In *Proceedings of the 2007 IEEE Radar Conference*. 385–390, Boston, USA: Institute of Electrical and Electronic Engineers.

[4] Kotik, D. S. and Itkina, M. A. (1998). On the physical limit of the power of heating facilities. *Journal of Atmospheric and Solar-Terrestrial Physics*, 60 (12), 1247–1256.

[5] Headrick, J. M. and Thomason, J. F. (1998). Applications of high-frequency radar. *Radio Science*, 33 (4), 1045–1054.

[6] Budden, K. G. (1985). The propagation of radio waves: the theory of radio waves of low power in the ionosphere and magnetosphere. Cambridge, UK: Cambridge University Press.

[7] Maclean, T. S. M. and Wu, Z. (1993). Radiowave propagation over ground. London: Chapman & Hall, p 230.

[8] Barrick, D. E. (1972). Remote sensing of sea state by radar. In V. E. Derr, (Ed.), *Remote sensing of the troposphere*, pp. 12.1–12.46. US Govt. Printing Office.

[9] International Radio Consultative Committee (1998). Characteristics and applications of atmospheric radio noise data. (CCIR Report 322-3). International Telecommunication Union.

[10] Booker, H. G. (1936). Oblique propagation of electromagnetic waves in a slowly-varying non-isotropic medium. *Proceedings of the Royal Society of London*, A. 155, 411–451.

[11] Tatarskii, V. I. (1961). Wave propagation in a turbulent medium. New York: Dover.

[12] Rufenach, C. L. (1975). Ionospheric scintillation by a random phase screen: spectral approach. *Radio Science*, 10 (2), 155–165.

[13] Coleman, C. J. (1996). A model of HF sky wave radar clutter. *Radio Science*, 31 (4), 869–875.

[14] Riddolls, R. J. (2006). A model of radio wave propagation in ionospheric irregularities for prediction of high-frequency radar performance. (DRDC Ottawa TM2006-284). Defence R&D Canada.

[15] Gherm, V. E., Zernov, N. N., and Strangeways, H. J. (2005). HF propagation in a wideband ionospheric fluctuating reflection channel: physically based software simulator of the channel. *Radio Science*, 40 (1), 1–15.

[16] Kelley, M. C. (1989). The earth's ionosphere. San Diego: Academic Press, p 151.

[17] Reed, I. S. (1962). On a moment theorem for complex Gaussian processes. *IRE Transactions on Information Theory*, 8 (4), 194–195.

[18] Barrick, D. E. (1982). Analysis methods for narrow-beam high-frequency radar sea echo. (NOAA Technical Report ERL 420-WPL 56). National Oceanic and Atmospheric Administration.

[19] Maresca, J. W. and Barnum, J. R. (1982). Theoretical limitation of the sea on the detection of low Doppler targets by over-the-horizon radar. *IEEE Transactions on Antennas and Propagation*, 30, 837–845.

[20] Barnum, J. R. (1986). Ship detection with high-resolution HF skywave radar. *IEEE Journal of Oceanic Engineering*, 11 (2), 196–209.

[21] Leong, H. and Ponsford, A. (2004). The advantages of dual frequency operation in ship tracking by HF surface wave radar. In *RADAR 2004 International Radar Conference Proceedings*. Toulouse, France.

Distribution list

DRDC Ottawa TM 2007-327

LIST PART 1: Internal Distribution by Centre

1 H/RS (Doreen Dyck)
1 GL/MFR/RS (David DiFilippo)
1 Hing Chan
1 Zhen Ding
1 Hank Leong
2 Ryan Riddolls
2 Library

9 TOTAL LIST PART 1

LIST PART 2: External Distribution by DRDKIM

1 ADM(S&T)
1 DGSTO
1 DRDKIM 3
1 CORA (Library)
1 DMRS 2
1 DSTM 3
1 DSTC4ISR
1 DJCP 4 (Cdr B. Houle)
1 D Mil CM 4 (LCol S. Murphy)
2 Library and Archives Canada (2 HC, 1 SC)

11 TOTAL LIST PART 2

20 TOTAL COPIES REQUIRED

This page intentionally left blank.

DOCUMENT CONTROL DATA

(Security classification of title, body of abstract and indexing annotation must be entered when the overall document is classified)

1. ORIGINATOR (the name and address of the organization preparing the document. Organizations for whom the document was prepared, e.g. Establishment sponsoring a contractor's report, or tasking agency, are entered in section 8.)

   Defence R&D Canada - Ottawa
   Ottawa, Ontario, K1A 0Z4

2. SECURITY CLASSIFICATION (overall security classification of the document, including special warning terms if applicable)

   UNCLASSIFIED

3. TITLE (the complete document title as indicated on the title page. Its classification should be indicated by the appropriate abbreviation (S,C or U) in parentheses after the title.)

   Ship Detection Performance of a High Frequency Hybrid Sky-Surface Wave Radar (U)

4. AUTHORS (Last name, first name, middle initial)

   Riddolls, Ryan J.

5. DATE OF PUBLICATION (month and year of publication of document)

   December 2007

6a. NO. OF PAGES (total containing information. Include Annexes, Appendices, etc.)

   34

6b. NO. OF REFS (total cited in document)

   21

7. DESCRIPTIVE NOTES (the category of the document, e.g. technical report, technical note or memorandum. If appropriate, enter the type of report, e.g. interim, progress, summary, annual or final. Give the inclusive dates when a specific reporting period is covered.)

   Technical Memorandum

8. SPONSORING ACTIVITY (the name of the department project office or laboratory sponsoring the research and development. Include the address.)

   Defence R&D Canada - Ottawa
   Ottawa, Ontario, K1A 0Z4

9a. PROJECT OR GRANT NO. (if appropriate, the applicable research and development project or grant number under which the document was written. Please specify whether project or grant)

   Project 11hh

9b. CONTRACT NO. (if appropriate, the applicable number under which the document was written)

10a. ORIGINATOR'S DOCUMENT NUMBER (the official document number by which the document is identified by the originating activity. This number must be unique to this document.)

   DRDC Ottawa TM 2007-327

10b. OTHER DOCUMENT NOS. (Any other numbers which may be assigned this document either by the originator or by the sponsor)

11. DOCUMENT AVAILABILITY (any limitations on further dissemination of the document, other than those imposed by security classification)

   (x) Unlimited distribution
   ( ) Distribution limited to defence departments and defence contractors; further distribution only as approved
   ( ) Distribution limited to defence departments and Canadian defence contractors; further distribution only as approved
   ( ) Distribution limited to government departments and agencies; further distribution only as approved
   ( ) Distribution limited to defence departments; further distribution only as approved
   ( ) Other (please specify):

12. DOCUMENT ANNOUNCEMENT (any limitation to the bibliographic announcement of this document. This will normally correspond to the Document Availability (11). However, where further distribution (beyond the audience specified in 11) is possible, a wider announcement audience may be selected.)

   Unlimited

13. ABSTRACT (a brief and factual summary of the document. It may also appear elsewhere in the body of the document itself. It is highly desirable that the abstract of classified documents be unclassified. Each paragraph of the abstract shall begin with an indication of the security classification of the information in the paragraph (unless the document itself is unclassified) represented as (S), (C), or (U). It is not necessary to include here abstracts in both official languages unless the text is bilingual).

(U) A high frequency radar configuration consisting of a skywave transmit path and a surface wave receive path is presented and analyzed. Limits on the radar resolution capability are determined using an analytic ray tracing formulation of radar signal propagation in an ionospheric plasma. This resolution is then substituted into the radar equation. It is found that the detection of low-velocity surface vessels is limited by ocean clutter. In this clutter-limited detection mode, it is found that the minimum observable vessel radar cross section (RCS) depends on the direction of the wind relative to the radar beam. At a surface wave range of 200 km, the minimum observable radar cross sections vary between 18 and 30 dBsm (daytime) and 30 and 42 dBsm (nighttime), as the wind direction varies from parallel to the radar beam to perpendicular. The minimum cross section also varies with the first power of range. During periods of spread F ionospheric turbulence the minimum detectable vessel RCS may increase by 20 dB.

14. KEYWORDS, DESCRIPTORS or IDENTIFIERS (technically meaningful terms or short phrases that characterize a document and could be helpful in cataloguing the document. They should be selected so that no security classification is required. Identifiers such as equipment model designation, trade name, military project code name, geographic location may also be included. If possible keywords should be selected from a published thesaurus. e.g. Thesaurus of Engineering and Scientific Terms (TEST) and that thesaurus-identified. If it is not possible to select indexing terms which are Unclassified, the classification of each should be indicated as with the title.)

HIGH FREQUENCY
RADAR
OVER THE HORIZON
SKY WAVE
SURFACE WAVE
MIXED MODE
HYBRID
SEA CLUTTER
SCATTERING
PLASMA
IRREGULARITIES

Defence R&D Canada

Canada's leader in Defence
and National Security
Science and Technology

R & D pour la défense Canada

Chef de file au Canada en matière
de science et de technologie pour
la défense et la sécurité nationale

www.drdc-rddc.gc.ca